Article

Depletion of HIV reservoir by activation of ISR signaling in resting CD4+T cells

ISR signaling activation

ATF4 - - - → GPX4 ⊣ **Ferroptosis**

HIV LTR

CHOP

HIV transcription

Apoptosis

IFIT1

Anti-viral IFIT signaling

Reservoir reduction

Dajiang Li, Lilly M. Wong, Yuyang Tang, ..., Nancie M. Archin, David M. Margolis, Guochun Jiang

guochun_jiang@med.unc.edu

Highlights

ISR activation not only disrupts latent HIV but also reduces HIV+ CD4+T cells

HIV reservoir reduction by ISR activation has minimal impacts on HIV negative cells

HIV reservoir reduction is caused by the activation of ATF4/CHOP and ATF4/IFIT signaling

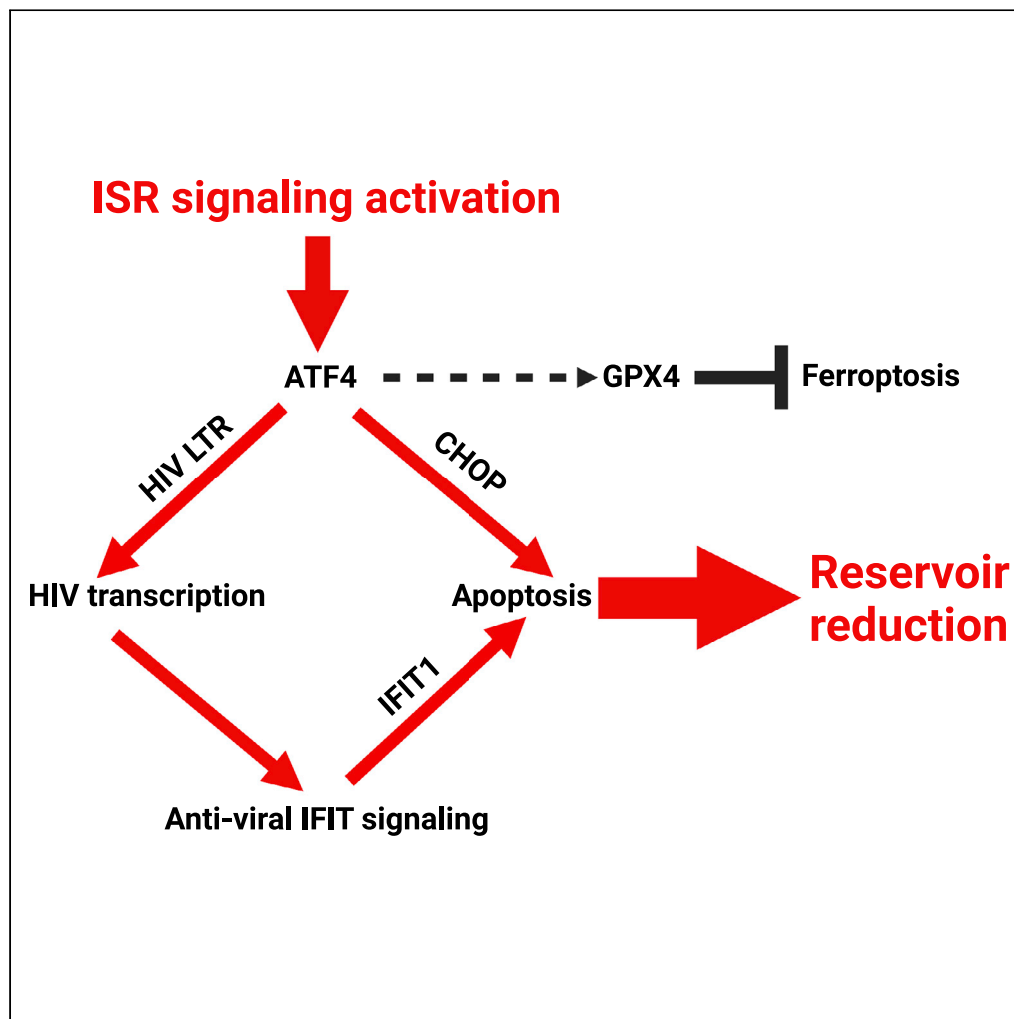ISR activation reduces replication-competent HIV in rCD4+ T cells from PLWH on ART

Article

Depletion of HIV reservoir by activation of ISR signaling in resting CD4+T cells

Dajiang Li,[1] Lilly M. Wong,[1] Yuyang Tang,[1] Brigitte Allard,[1] Katherine S. James,[1] George R. Thompson,[2] Satya Dandekar,[2] Edward P. Browne,[1,6] Qingsheng Li,[3] Jeremy M. Simon,[4] Nancie M. Archin,[1] David M. Margolis,[1,5,6] and Guochun Jiang[1,7,8,*]

SUMMARY

HIV reservoirs are extremely stable and pose a tremendous challenge to clear HIV infection. Here, we demonstrate that activation of ISR/ATF4 signaling reverses HIV latency, which also selectively eliminates HIV+ cells in primary CD4+T cell model of latency without effect on HIV-negative CD4+T cells. The reduction of HIV+ cells is associated with apoptosis enhancement, but surprisingly is largely seen in HIV-infected cells in which gag-pol RNA transcripts are detected in HIV RNA-induced ATF4/IFIT signaling. In resting CD4+ (rCD4+) T cells isolated from people living with HIV on antiretroviral therapy, induction of ISR/ATF4 signaling reduced HIV reservoirs by depletion of replication-competent HIV without global reduction in the rCD4+ T cell population. These findings suggest that compromised ISR/ATF4 signaling maintains stable and quiescent HIV reservoirs whereas activation of ISR/ATF4 signaling results in the disruption of latent HIV and clearance of persistently infected CD4+T cells.

INTRODUCTION

The extremely stable human immunodeficiency virus-1 (HIV) latent reservoir is a formidable obstacle to the cure of HIV infection.[1,2] Understanding the molecular basis behind HIV latency is of great importance to aid in the efforts to eradicate HIV infection in people living with HIV (PLWH). In the last decades, progress has been made, profoundly changing our view of HIV latency.[2–4] Accordingly, many approaches have been proposed, including "Kick and Kill", deep silencing, gene therapy and immune therapy, where some proposals have been tested in model systems.[3,5–7] The goal of these strategies is to significantly reduce the reservoir size to a level such that HIV rebound after antiretroviral therapy interruption will be greatly delayed, or even prevented altogether. Recently, inhibitor of apoptosis inhibitors (IAPi) has demonstrated potential as a new generation of latency reversal agents that directly activate the non-canonical NF-κB signaling pathway.[8,9] Unfortunately, although latency reversal agents have advanced, few approaches to effectively clear HIV reservoir have been achieved *in vivo,* indicating that alternatives are needed.

Host integrated stress response (ISR) serves as a trigger for the innate immune response in which the host translation machinery is temporarily blocked though eIF2/ATF4 signaling,[10,11] preventing pathogen infection unless ISR is abrogated by the dephosphorylation of eIF2 by protein phosphatase 1 (PP1) and its regulatory subunit GADD34 or CReP protein.[12] Previously, we found that ISR activation is active in acute but not chronic SIV infection.[11] Intriguingly, we also showed that ISR downstream signaling protein ATF4 serves as a transcription factor of HIV, hijacking ISR signaling to promote viral replication.[11,13] Recent studies have established that activation of ISR/ATF4 also induces autophagy.[12] Nevertheless, when ISR is not terminated by host control mechanisms, ATF4 induces transcriptional activation of apoptotic genes such as CHOP, and cell death is then triggered.[14] Many studies focus on the enforcement of ISR activation for cancer therapy. For instance, HA15, an ISR specific agonist of BIP (or GRP78) directly activates ISR/ATF4 signaling and induces tumor cell death.[15]

Here, we sought to investigate whether ISR/ATF4 signaling is involved in the persistent HIV infection in primary CD4+T cells.

[1]UNC HIV Cure Center, Institute of Global Health and Infectious Diseases, the University of North Carolina at Chapel Hill, Chapel Hill, NC 27599-7042, USA

[2]Department of Medical Microbiology, the University of California at Davis, Davis, CA 95616, USA

[3]School of Biological Sciences and Nebraska Center for Virology, the University of Nebraska-Lincoln, Lincoln, NE 68588-0118, USA

[4]Department of Genetics, the University of North Carolina at Chapel Hill, Chapel Hill, NC 27599-7042, USA

[5]Department of Microbiology and Immunology, UNC Neuroscience Center, the University of North Carolina at Chapel Hill, Chapel Hill, NC 27599-7042, USA

[6]Department of Medicine, the University of North Carolina at Chapel Hill, Chapel Hill, NC 27599-7042, USA

[7]Department of Biochemistry and Biophysics, the University of North Carolina at Chapel Hill, Chapel Hill, NC 27599-7042, USA

[8]Lead contact

*Correspondence: guochun_jiang@med.unc.edu

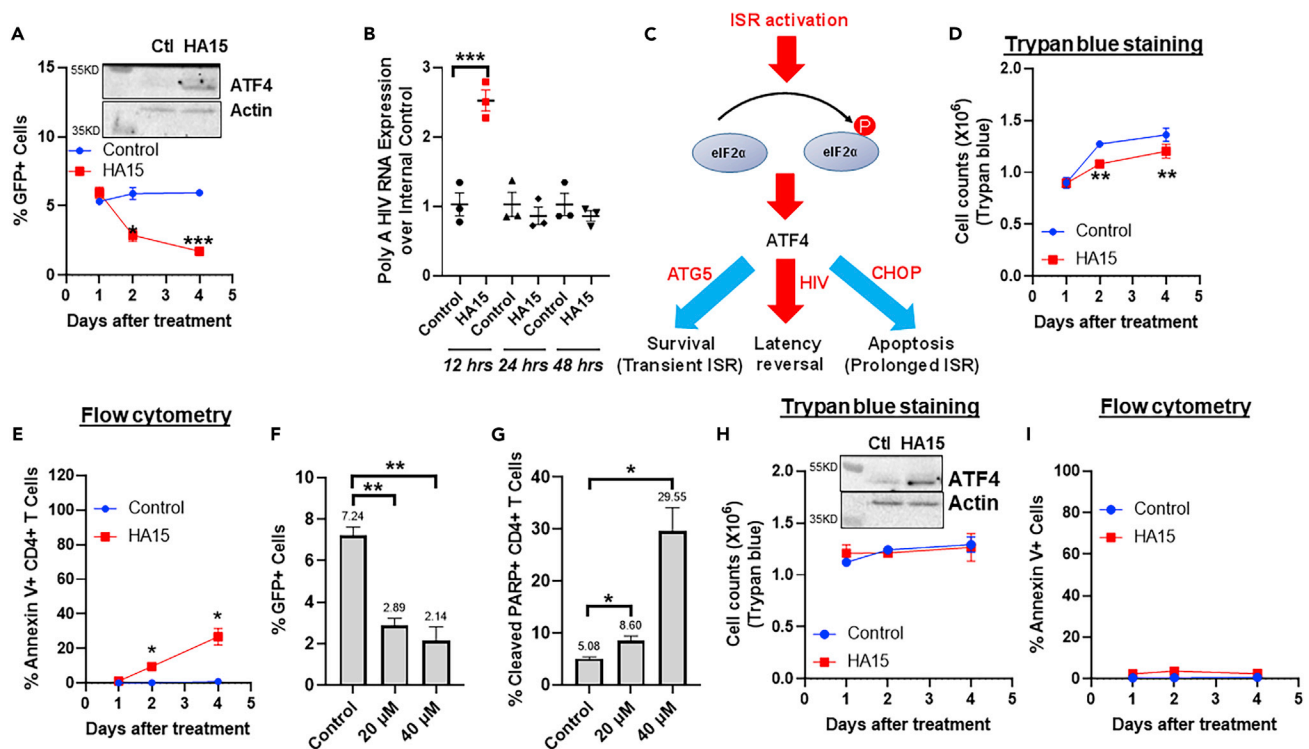https://doi.org/10.1016/j.isci.2022.105743

Figure 1. Activation of ISR disrupts latent HIV and reduces HIV+ cells in the primary CD4+T cell model of latency with minimal impact in bystander CD4+ T cells

The primary CD4+T cell model of HIV latency was treated with or without HA15. Cells were collected 12 h, 1 day, 2 days and 4 days after treatment. Percentage of GFP+ cells was analyzed by flow cytometry (A). HIV RNA was analyzed by qPCR (B). Protein expression of ATF4 was measured 24 h after treatment where actin served as loading controls (insert in A). Proposed ISR/ATF4 downstream signaling was shown in (C). Total cell number was counted with Trypan blue staining (D). while flow cytometry was performed to analyze cell apoptosis (Annexin V) (E). Similar as in A-B, the primary CD4+T cell model of latency was treated with 20 or 40 μM HA15, and cells were collected 4 days after treatment. Flow cytometry was performed to analyze HIV expression (GFP), cell apoptosis (cleaved PARP1) and viability (F and G). Then, HIV negative primary CD4+T cells were treated with 20 μM HA15. Cells were collected 1 day, 2 days and 4 days after treatment. ATF4 protein expression are analyzed 2 days after 20 μM HA15 treatment (G, insert) whereas total cell number was counted with Trypan blue staining (G). Flow cytometry was performed to analyze cell apoptosis (Annexin V) and viability (I). *, p<0.05; *, p<0.01; ***, p<0.001; ****, p<0.00001, analyzed with one-way ANOVA or two-tailed t test compared with the control treatment (n = 3).

RESULTS

Activation of ISR disrupts latent HIV in Jurkat models of HIV latency

We initially tested the impact of ISR/ATF4 activation in Jurkat models of HIV latency (J-Lat A1 and 2D10 cells) in which GFP expression represents HIV transcription or latency reversal. One day post-treatment, ISR downstream protein ATF4 was highly induced where the percentage of GFP positive cells was increased (Figures S1A–S1D). Cell viability was slightly decreased when 40 μM HA15 was added, which is indicative of cellular toxicity. Similarly, in the 2D10 model of HIV latency, two days post HA15 treatment, up to 50% cells were GFP+ (Figures 1 SE–1H). Like J-Lat A1 cells, viability of 2D10 cells was reduced (∼10%) at high concentrations of HA15 (Figure S1H). At the transcriptional level, HA15 elicited a dose-dependent induction of both ATF4 and HIV expression (Figure S1). These data suggest that, consistent with our previous report and other observations,[11,13] activation of ISR/ATF4 signaling reverses HIV latency in Jurkat models of HIV latency. Because global cellular toxicity was observed at 40 μM HA15, most of the following studies utilized 20 μM HA15.

Prolonged activation of ISR reduces HIV+ cells in the primary CD4+T cell model of latency

We next examined whether the activation of ISR/ATF4 induces HIV transcription from latency in the primary CD4+T cell model of latency, which was established and cultured as described.[16,17] Briefly, primary CD4+T cells from HIV negative donor were infected with pNL4.3Δ6-GFP. Then, GFP+ cells were sorted by flow cytometry and continue to co-culture with H80 cells, a feeder cell line to maintain cell growth and allow the

establishment of HIV latency.[18] Lastly, GFP- CD4^{+}T cells were sorted out to use as the primary CD4^{+}T cell model of HIV latency.[16,17]

ATF4 was induced one day post HA15 treatment (Figure 1A, insert); however, no increase of GFP expression was observed (Figure 1A). Surprisingly, in contrast to Jurkat models of HIV latency where the treatment was continued for 2 days, the frequency of GFP+ cells was reduced by 51%. Four days after HA15 treatment, the percentage of GFP+ cells further decreased (71% reduction; Figure 1A). When HIV transcription was directly measured, we found that HIV RNA significantly increased 12 h after HA15 treatment but returned to its baseline after 24 h (Figure 1B). These data suggest that although HIV transcription was induced across all model systems studied, the primary cell model exhibits transient HIV transcription, followed by loss of GFP+ cells upon prolonged ISR/ATF4 activation by HA15 unlike Jurkat models of HIV latency.

Activation of ISR signaling modestly induces apoptosis to deplete HIV+ cells in HIV latently infected primary CD4^{+}T cells but not HIV-negative primary CD4^{+}T cells

Activation of ISR signaling results in ATF4 expression and activation of ATF4-dependent gene expression, such as CHOP, GADD34, CReP and HIV.[11–13] Transient ISR signaling induces autophagy to protect cells for survival, whereas prolonged ISR signaling triggers cell death (Figure 1C).[14] We explored the cause of HIV+ cell death in the primary CD4^{+}T cell model of latency after exposure to HA15. We measured cell apoptosis and cellular viability among these latency models by trypan blue staining and flow cytometry. We reasoned that trypan blue staining may give us an overview of cellular viability and cell death, as flow cytometry often underestimates cell death. In addition, to directly analyze cell death, we measured annexin V+ (early death marker) and cleaved PARP1+ (late death marker) cells during flow cytometry. The total cell number was slightly reduced (Figure 1D) whereas the Annexin V+ cells increased up to 26.8% during the four-day treatment (Figure 1E), indicating an induction of cell death after ISR/ATF4 signaling activation. This was similarly observed in the late-stage apoptosis with cleaved-PARP1 flow cytometry assay in which 8.6% of cells were cleaved-PARP1+. The percentage of cleaved-PARP1+ cells further increased to 29.55% when a higher dosage of HA15 (40 μM) was applied to the cells (Figures 1F and 1G). Taken together, these data suggest that prolonged ISR activation induces cell death to deplete HIV+ cells in the primary CD4^{+}T cell model of HIV latency.

Surprisingly, in HIV-negative CD4^{+}T cells, activation of ISR/ATF4 signaling by 20 μM HA15 treatment did not reduce the total number of CD4^{+}T cells measured by trypan blue staining (Figure 1H). This is likely because of minimal induction of cell apoptosis in CD4^{+}T cells without HIV infection (Figure 1I).

To study the ISR/ATF4 signaling in both HIV+ and HIV negative primary CD4^{+}T cells, we measured ISR/ATF4-associated death (Caspase3 cleavage) or autophagy (LC3B cleavage) signaling activation by Western blot. We found that ATF4 and CHOP proteins were induced in both cell types (Figure 2). Although cell apoptosis was transiently induced in primary CD4^{+}T cell latency model (HIV+), minimal cell death was induced in HIV-negative primary CD4^{+}T cells. In HIV-negative primary CD4^{+}T cells, autophagy was activated by ISR/ATF4 activation 1 day after treatment then reduced to the basal level. Minimal LC3B cleavage was observed in primary CD4^{+}T cell model of latency even at a higher concentration of HA15 was added. These data indicate that activation of ISR signaling may selectively induce cell death, but not autophagy, in the HIV+ CD4^{+}T cells without significant impact on apoptosis in the HIV negative CD4^{+}T cells.

Minimal cell death is induced by HA15 treatment in the resting CD4^{+} T (rCD4+) cells isolated from ART-suppressed PLWH

Extremely low levels of HIV+ cells exist in the rCD4+ T cells isolated from ART-suppressed PLWH. We therefore reasoned that ISR activation may not induce severe cellular toxicity in these rCD4+ T cells. As expected, the total cell number of rCD4+ T cells did not change after 20 μM HA15 treatment, nor did it induce toxicity in these cells (Figures 3A and 3B). Similar to the HIV-negative primary CD4^{+}T cells, very low levels of Annexin V was induced (Figure 3C), indicating that a minimal level of cell apoptosis was induced. Taken together, these data from primary CD4^{+}T cell model of latency, HIV negative CD4^{+}T cells and the rCD4+ T cells from PLWH suggest that HA15 may selectively reduce HIV+ cells without impact on bystander CD4^{+}T cells.
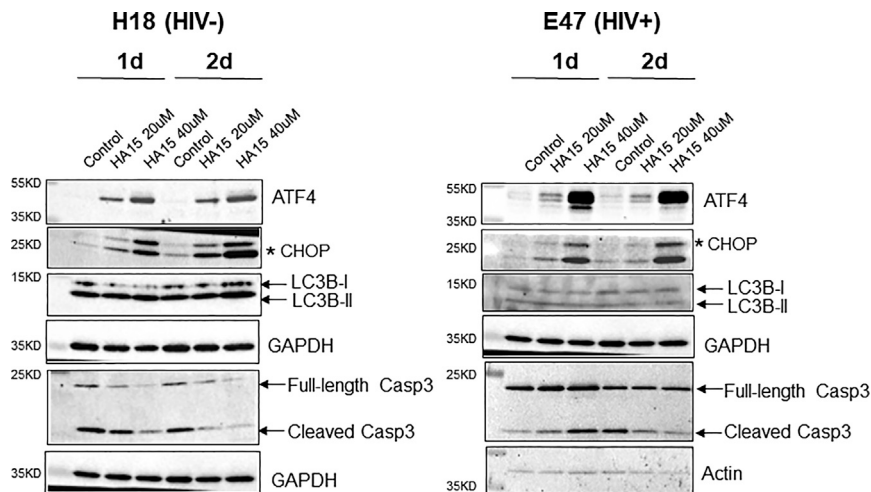
Figure 2. ISR/ATF4 signaling activation in T cells with or without latent HIV infection

HIV negative primary CD4$^+$T cells (H18) or primary CD4$^+$T cell models (E47) of latency were treated with 20 or 40 μM HA15 for 1–2 days. Cells were collected. Then, the whole cell protein lysates were prepared and subjected to Western blot to measure the protein expression in ISR/ATF4 pathways. *, band of CHOP protein.

Ex vivo ISR/ATF4/CHOP activation reduces HIV proviral DNA in rCD4+ T cells isolated from ART-suppressed PLWH

Previously, we found that ISR/ATF4 induced SIV transcription while ISR signaling was activated in the acute but not in chronic SIV infection of rhesus macaques.[11] Others reported that ISR activation is associated with latency reversal or HIV transcription via the induction of ATF4. Of interest, the expression of ATF4, but not eIF2α or its kinase, EIF2AK4 (or GCN2), correlated with a reciprocal decline of SIV viral loads in the intestine *in vivo*[11] (Figures 3D, S2A, and S2B). These observations point to an idea that suppression of ISR/ATF4 signaling is associated with HIV latency[13] whereas enforced ISR/ATF4 activation may be able to reduce HIV reservoirs *in vivo*. To test this hypothesis, four days after 20 μM HA15 treatment, total RNA was extracted from the primary CD4$^+$T cells isolated from ART-suppressed PLWH. We found that HA15 activated ISR and induced ATF4 and its downstream target CHOP (Figures 3E and 3F). We also studied the expression of autophagy genes including ATG5 and ATG7. However, minimal impact was observed in patient CD4$^+$T cells in the presence of HA15 (Figures S2C and S2D).

The induction of ATF4/CHOP signaling in the patient cells support our observations in the primary CD4$^+$T cell model of latency. In fact, we found that HIV DNA was reduced (up to 19.27-fold reduction) 4 days post-treatment of 20 μM HA15 in all patient rCD4+ T cells on ART (Figure 3G). Taken together, these data indicate that the inactivation of ISR/ATF4 is associated with the persistence of HIV reservoir. When activated or enforced, ISR/ATF4 signaling can disrupt latency and reduce HIV reservoirs.

Ex vivo ISR/ATF4/CHOP activation reduces replication competent HIV to deplete HIV reservoir in rCD4+ T cells isolated from ART-suppressed PLWH

Reduction of HIV proviral DNA may not lead to the depletion of HIV reservoirs because most of the proviruses in PLWH are replication-incompetent. To this end, a viral outgrowth assay was carried out in rCD4+ T cells isolated from PBMCs of ART-suppressed PLWH (n = 5) for 21 days (Figure 4A). We found that activation of ISR/ATF4 signaling by 20 μM HA15 reduced both cell-associated outgrowth HIV RNA (up to 340-fold reduction) and outgrowth HIV DNA (up to 2378-fold reduction) among all patient samples (Figures 3B and 3C). Notably, HIV in the outgrowth cell culture supernatants was also depleted in all the tested samples (up to 1917-fold reduction) (Figure 3D).

Taken together, these observations strongly suggest that ISR/ATF4 activation reduced replication-competent HIV in the rCD4+ T cells with minimal cellular toxicity.
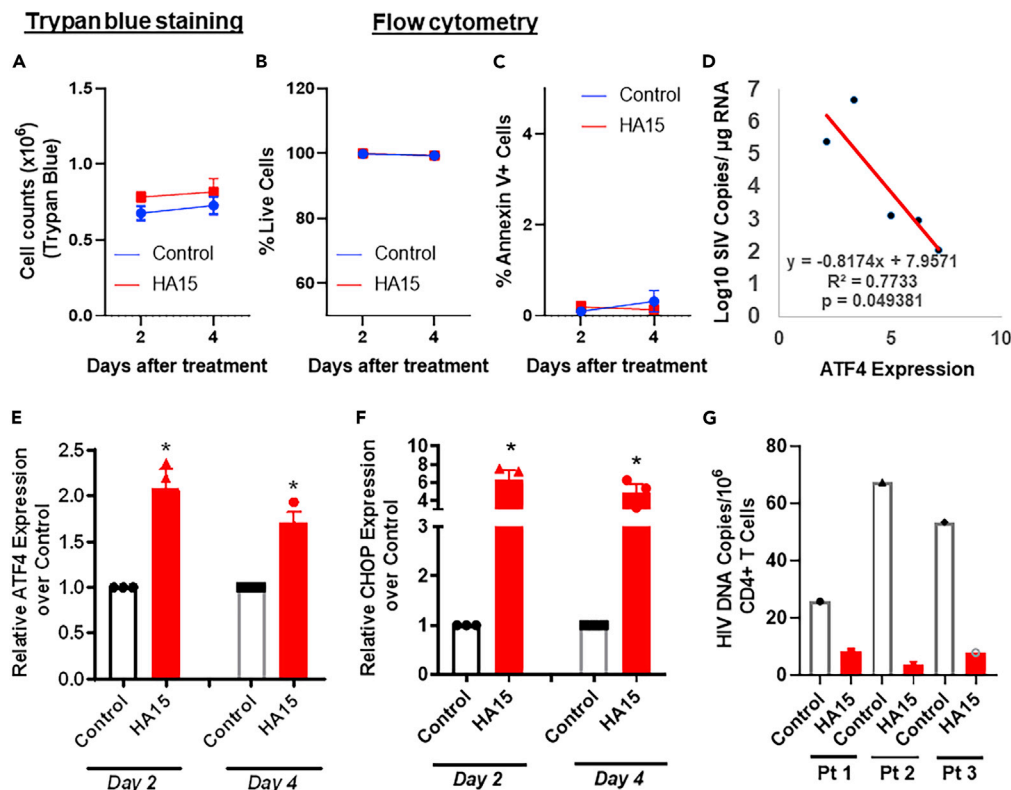
Figure 3. Activation of ISR signaling reduces HIV DNA/RNA without impact on global cell number of rCD4+ T cells isolated from PLWH on ART

The rCD4+ T cells isolated from ART-suppressed PLWH (n = 4) were treated with 20 μM HA15. Cells were collected 1 day, 2 days and 3 days after the treatment (n = 3). Total cell number was counted with Trypan blue staining.

(A–C) Trypan blue staining and flow cytometry were performed to analyze cell viability and apoptosis (Annexin V).

(D) Total RNA was extracted from the intestinal tissues in the SIV acutely infected rhesus macaques (n = 5). ATF4 gene expression and SIV RNA were quantitated by qRT-PCR. Then, the correlation of gene expression in the same animals was analyzed by linear regression.

(E and F) Patient primary CD4$^+$T cells were treated with DMSO or 20 μM HA15 for 4 days. Then, the expression of ATF4 and CHOP was measured by RT-qPCR.

(G) Resting CD4$^+$T cells (n = 3) were treated with or without 20 μM HA15 for 4 days. Cells were collected, then HIV *env* DNA was extracted and subjected for droplet digital PCR (ddPCR) (n = 3). *, p<0.05, analyzed with two-tailed *t* test compared with the control treatment (n = 3).

Targeting ISR/ATF4 negative feedback enhances the reduction of GFP+ cells elicited by HA15 induction in the primary CD4$^+$T cells model of latency

Activation of ISR/ATF4 signaling also elicits negative regulatory feedback to prevent excessive stress signaling to protect cells from cell death. This is achieved by the induction of PP1 cofactor GADD34 or CReP to de-phosphorylate eIF2α, thereby blocking ATF4 translation[12] (Figure 5A). It has been shown that Sephin1 or the HIV protease inhibitor (PI) ritonavir inhibits GADD34/CReP to cure cancer.[19,20] Therefore, we hypothesized that ISR/ATF4 signaling could be further enhanced by breaking the negative feedback loop. We found that targeting eIF2 by ritonavir, but not Sephin1, did enhance the reduction of GFP+ cells. HA15 (20 μM) treatment alone reduced 47% of GFP+ cells, co-treatment of HA15 with Ritonavir further decreased 80% of GFP+ CD4$^+$T cells (Figures 5B and 5C), which may be associated with the induction of cell death in the presence of dual targeting in ISR/ATF4 signaling (Figure 5D). Because the primary CD4$^+$T cell model of latency was infected by pNL4.3-Δ6-GFP in which no HIV protease but only HIV Tat and Rev are expressed, the enhancement of GFP+ cell reduction is not related to the inhibition of HIV maturation by ritonavir, indicating that GFP+ cell reduction may be solely due to the cell death effect of ISR/ATF4 signaling enhancement. Together, these data suggest that HIV reservoirs can be further reduced when eIF2/PP1 regulatory feedback is targeted.
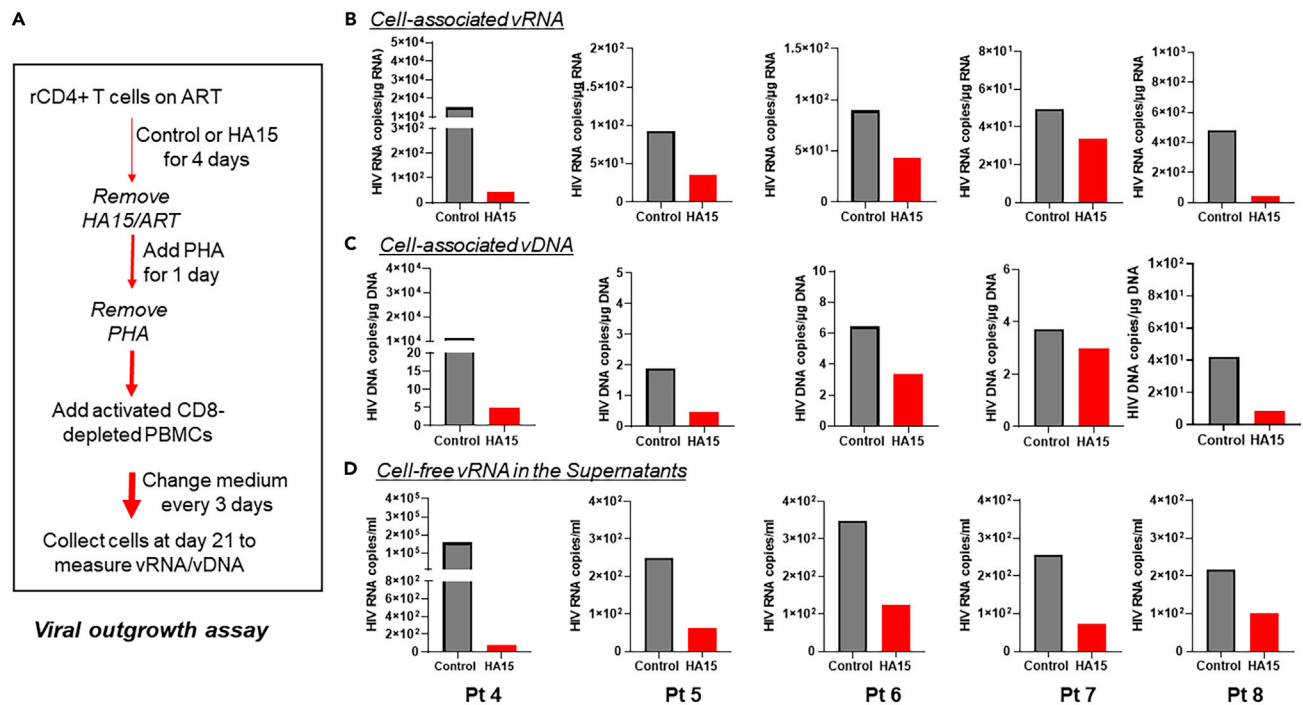
Figure 4. Activation of ISR signaling depletes replication competent HIV in the rCD4+ T cells isolated from PLWH on ART

(A) Resting CD4$^+$T cells were treated with or without 20 μM HA15 for 4 days in the presence of ART plus 20 U/mL IL-2 (n = 5). Then, the treatment was washed out, followed by PHA (2 μg/mL) reactivation for 24 h. PHA was then washed out and cells were co-cultured with CD8-depleted human PBMCs to measure viral outgrowth. Cells were collected 21 days after co-culture with CD8-depleted human PBMCs.

Cell and supernatants were collected. (B–D) Cell-associated HIV gag RNA, HIV gag DNA and cell-free HIV gag RNA were determined by RT-ddPCR and/or ddPCR.

HA15-induced cell death mainly occurs in HIV RNA+ cells in primary CD4$^+$T cell model of latency

HA15-induced ISR/ATF4 signaling is associated with the reduction of HIV reservoirs in which HIV RNA was transiently increased then reduced (Figure 1B). This led us to explore whether ISR/ATF4 activation-induced HIV RNA contributes to the reduction of HIV+ cells. With HIV RNA FISH-Flow analyses[21] (Figures 6A and 6B), we found that HA15 (20 μM) significantly increased cleaved-PARP1+ cells. Consistent with our hypothesis, HIV RNA+/cleaved PARP1+ (i.e., apoptosis+) cells were significantly more prevalent after HA15 treatment (7.20%) compared to control treatment (2.01%) (Figures 6C and 6D). Of interest, there was a significant portion of cleaved PARP1+ cells in the HIV RNA negative population of CD4$^+$T cells (5.51%) (Figure 6E). Notably, the percentage of HIV RNA+/cleaved PARP1+ cells was significantly higher than those in HIV RNA-/cleaved PARP1+ cells (p = 0.0054, n = 5). Taken together, HIV viral RNA induction by ISR/ATF4 activation may contribute to the depletion of HIV reservoirs via the induction of cell death.

Single cell RNA-seq identifies signaling pathways associated with HIV+ cell reduction in the primary CD4$^+$T cell model of latency

To better understand the mechanisms of HIV+ cell reduction, we carried out single-cell RNA-seq (scRNA-seq) analyses in control and HA15 (20 μM)-treated primary CD4$^+$T cell model of latency 2 days posttreatment. Overall, the CD4$^+$T cells clustered distinctly into 8 groups where clusters 0–3 contained most of the cells, regardless of treatment groups (Figure S3). Within each cluster, HA15-treated cells were distinct from the control-treated cells, indicating that HA15 treatment is associated with an altered transcriptome in the primary CD4$^+$T cell model of latency. The experimental strain of pNL4-3-Δ6 contains 6 mutations, in which only HIV Tat and Rev proteins are expressed.[16] In fact, Tat and Rev RNA transcripts were detectable in many of the cells assayed (Figure 7A). Of interest, the pattern of Tat and Rev expressions across the eight clusters was similar. This gave us an opportunity to separate putative HIV+ (i.e., Tat+/Rev+) cells from putative HIV- (i.e., Tat-/Rev-) cells (Figure S4A) although, interestingly, transcription of Rev was detected in more clusters of cells than Tat (Figure S4B). Even though HIV Tat and Rev were mostly transcriptionally active
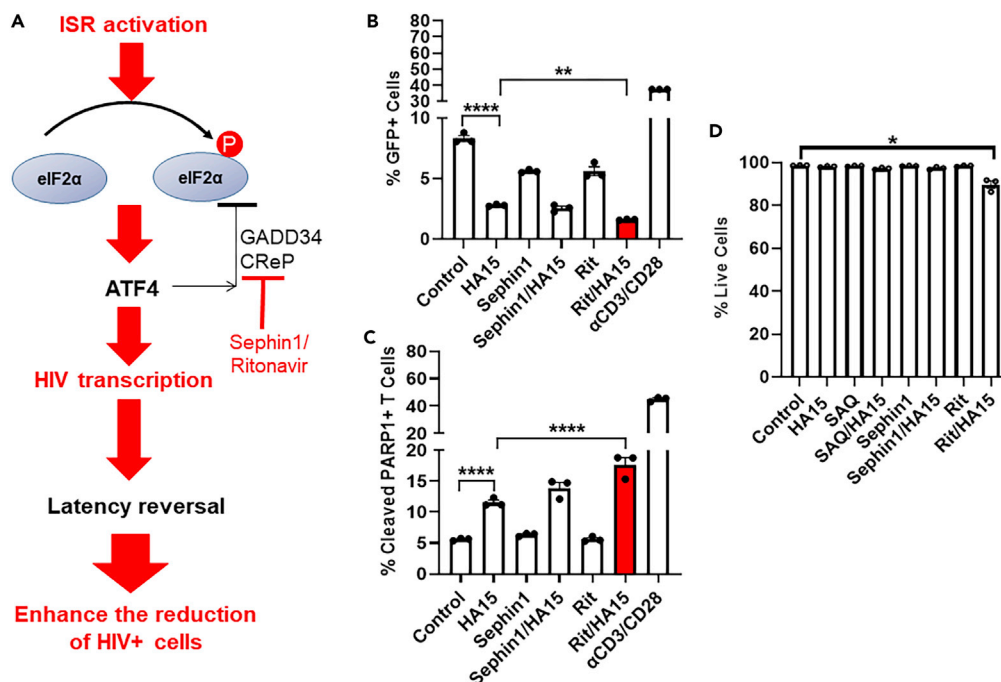
Figure 5. Targeting eIF2α/GADD34/CReP by Ritonavir enhances the reduction of GFP+ cells elicited by HA15 in the primary CD4+T cell model of latency

Model of ISR/ATF4 signaling pathway to activate HIV and induce cell death which is negatively regulated by ATF4-induced gene GADD34 and HIV protease. Breaking these negative feedback loops by the inhibition of GADD34 by Sephin 1 or HIV protease by Ritonavir (Rit) may enhance the cell death in HIV+ CD4+T cells.

(A) Primary CD4+T cell model of latency was treated with 20 μM HA15, 20 μM Sephin-1, 10 μM Rit alone or in combination. (B–D) Anti-CD3/CD28 treatment was used as a positive control. Cells were collected 4 days after treatment, and the percentage of GFP positive cells and cellular viability were analyzed by flow cytometry. *, p<0.05; **, p<0.01; ****, p<0.0001 (n = 3). Data were analyzed by One-way ANOVA.

(Figure 7A), ~95% cells were translationally inactive[17] (Figure 1). These observations indicate that a defective translation machinery is associated with HIV quiescence in this primary CD4+T cell model of latency.

We then compared the expression profiles of HA15-treated and control-treated cells within each of the eight cell clusters identified (Data S1) and looked for evidence of ISR/ATF4 signaling activation. Indeed, *ATF4* was significantly upregulated in HA15-treated cells in Clusters 0, 2, 3, and 5, and CHOP (known as *DDIT3*) was also upregulated in Clusters 2 and 3. We then repeated the differential expression testing on putative HIV+ and putative HIV- cells separately for each cluster (Data S2) and performed a pathway over-enrichment analysis. With this approach, we could specifically look for effects related to cell death or apoptosis, translation, stress or stimulus response or similar pathways, and ask whether their expression changes were unique depending on treatment or HIV status (Figure 7B). As expected, we found that pathways related to translation, ER (i.e., ISR), and stress response were frequently modulated by HA15, and many of these were commonly upregulated in both HIV+ and HIV- cells. Cell death and apoptosis pathways were among the common downregulated pathways in HA15-treated cells, and seemingly was more frequently significant among HIV- cells. This may be because this pathway is largely controlled by post-translational protein degradation, such as caspase or PARP1 cleavage, which may not be fully captured at the transcriptional level by scRNA-seq, or because there were more HIV- cells overall and thus increased statistical power to detect differential expression. Notably, innate immunity pathways were also significantly modulated, which may be elicited by a transient HIV RNA induction after IAR/ATF4 activation by HA15 (Figure 1B).

Lastly, in addition to canonical cell death and apoptosis pathways, we also detected a significant enrichment of genes that were differentially expressed and participated in the ferroptosis signaling pathway. Expression of *GPX4, FTH1, FTL,* and *SLC3A2* was highly induced following HA15 treatment across many
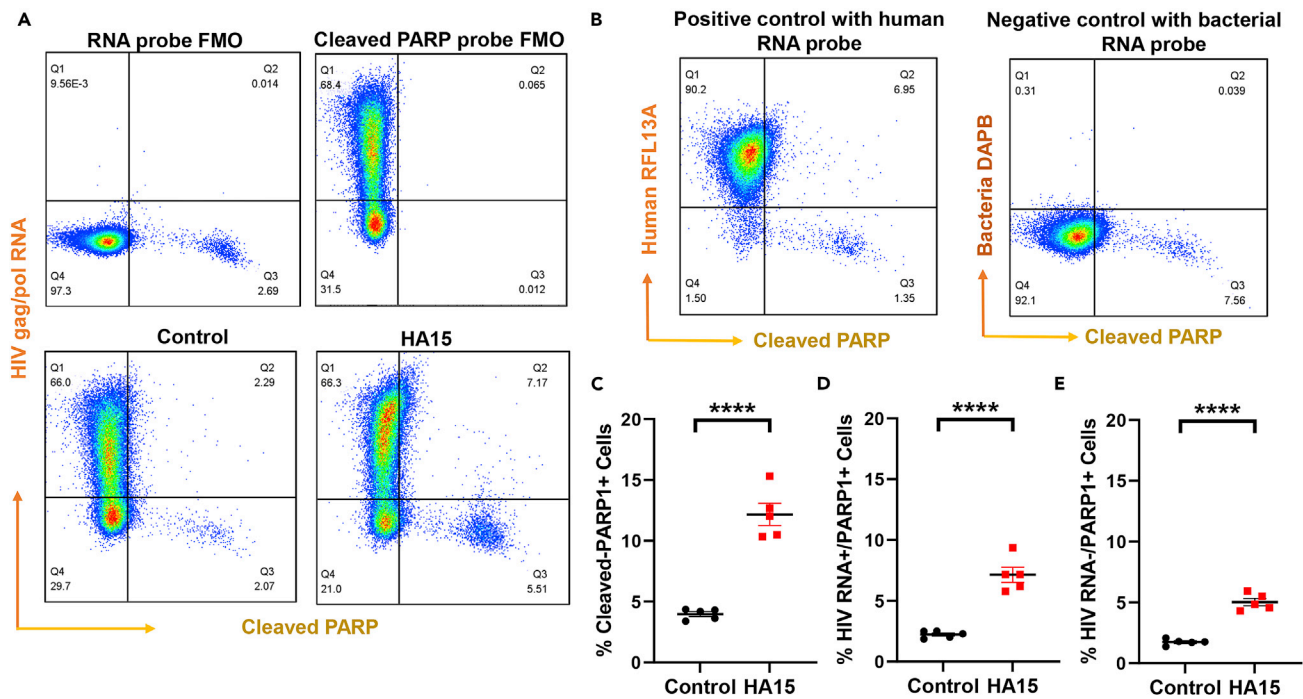
Figure 6. ISR/ATF4 activation by HA15 treatment enhances cleaved PARP in HIV RNA+ cells in the primary CD4⁺T cell model of latency

Primary T cell model were treated with or without HA15 (20 μM) for 2 days. Cells were collected and prepared for HIV RNA FISH-Flow. Flow gating strategy and representative flow charts of HIV RNA and cleaved PARP staining from the treated or untreated cells.

(A) Positive control (probe for Human RFL13A) and negative control (probe for Bacteria DAPB) cells during the flow cytometry.

(B) Percentages of cleaved PARP1+ cells and cleaved PARP1+ cells in RNA+ or HIV RNA-cells with or without ISR/ATF4 activation.

(C–E). ****, p<0.0001 analyzed by two-tailed T-test.

of the clusters (Figure S5 and Data S2). Deficiency of these genes are critical for the induction of a unique cell death signaling, ferroptosis,[22–24] indicating that ISR/ATF4 signaling may regulate these genes to suppress ferroptosis, serving as a previously unrecognized negative feedback for the survival of quiescent CD4⁺T cells harboring latent HIV.

Anti-viral IFIT signaling is induced by HA15 and is associated with cell death in HIV RNA+ cells in primary CD4⁺T cell model of latency

Activation of innate immune response identified by scRNA-seq (Figure 7) prompted us to further examine the role of this pathway in the reduction of HIV+ cells. HA15 is a derivative of a thiazolide family compound.[15] Of interest, it has been reported that thiazolides inhibited HIV replication via stimulation of anti-viral type I IFN (IFN-I) signaling,[25] which is known to block HIV transcription, translation, and/or subsequently induce cell death,[26] suggesting a potential link of anti-viral innate immune response to HIV+ cell reduction supported by our scRNA-seq analysis. In fact, in the primary CD4⁺T cell model of HIV latency, RIG-I and IFIT1 were significantly upregulated 24 h after HA15 (20 μM) treatment whereas IFIT2 was upregulated after treatment for 48 h. Other IFN-I signaling genes, were also analyzed, including STAT1, STAT2, STAT3, MDA5, MyD88, IRF3 and IRF7 and the restrictive factor SAMHD1, but no significant change was observed (Figures 8A and S6). Notably, NOD2, TLR3, TLR7, IFNα and IFNβ genes were not detected (not shown) in the primary CD4⁺T cell model of HIV latency.

Induction of IFITs after ISR/ATF4 activation led us to investigate whether IFIT signaling is involved in the reduction of HIV reservoirs because IFITs are well-defined to block viral RNA translation and induce cell death of infected cells.[27–29] Therefore, we analyzed IFIT1 expression in CD4⁺T cells in the primary CD4⁺ T cell model of HIV latency and found that the percentage of IFIT1+ cells was significantly enhanced after ISR/ATF4 activation by HA15 (20 μM) (Figure 8B). Importantly, RNA FISH-Flow showed that the percentage of HIV RNA+ (gag-pol RNA+)/IFIT1+ cells was markedly increased after ISR/ATF4 activation (4.2-fold from 1.52 to 6.48%). Importantly, in gag-pol RNA+/IFIT1+ cells, cleaved PARP1 cells were increased from 0.76 to
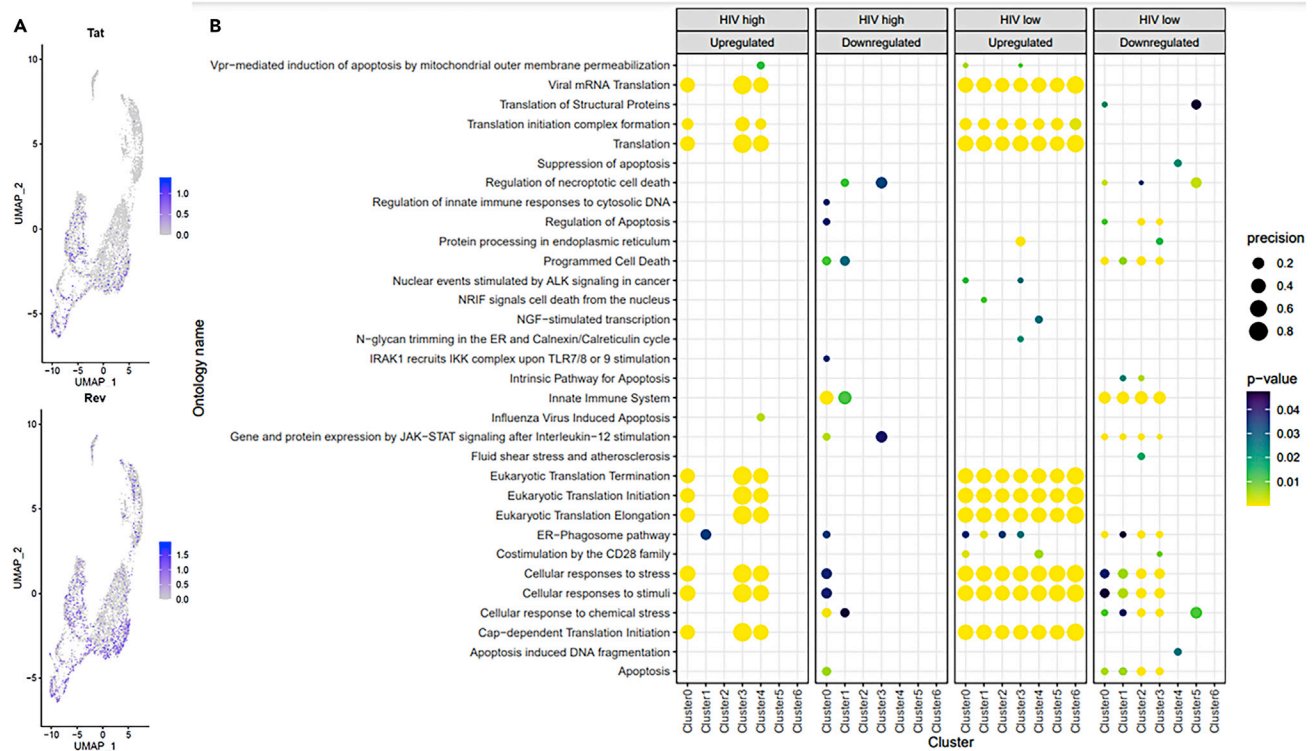
Figure 7. Single cell RNA-seq analysis identifies major modulated pathways that related to HIV+ cell reduction after ISR activation by HA15 in primary CD4⁺T cell model of latency

(A) The transcription of HIV Tat and Rev across all cells plotted in two-dimensional UMAP space. SCT-normalized expression data are plotted, higher expression is indicated in purple.

(B) Cells were treated with or without HA15 for 2 days, then the cells were collected for scRNA-seq analysis. Enriched gene ontology terms related to cell death or apoptosis, translation, stress or stimulus response, innate immunity, or similar pathways were plotted depending on treatment and HIV status. FDR <0.05 was considered significant.

5.20% (∼6.83-fold) (Figures 8C and 8D), indicating that HIV RNA/IFIT1 innate immune signaling may play a role in the induction of cell death after ISR/ATF4 activation.

To our surprise, in the transformed cell-derived Jurkat HIV latency model (2D10), the transcription profile was nearly opposite to the primary CD4⁺T cell model of latency in which HIV transcription was not induced until 48 h after induction by ISR activation by 20 μM HA15 (Figure S7A). Also, opposite to the primary CD4⁺T cell model of latency (Figure 8), the expression of innate immune genes, such as RIG-I, IFIT1, IFIT2, STAT1 and STAT2, was not enhanced. Instead, the expression of IFIT1 was reduced 24 or 48 h after HA15 treatment (Figure S7B). This dysregulated IFIT signaling may be responsible for the continued increase of HIV transcription in Jurkat model of latency because IFIT signaling is impaired. In contrast, because the anti-viral IFIT signaling is intact and induced in the primary CD4⁺T cells of latency after ISR/ATF4 activation, it may control the transient HIV transcription and subsequent induction of apoptosis, leading to the reduction of HIV+ cells to deplete HIV reservoir in CD4⁺T cells (Figure S7C).

DISCUSSION

Here, we showed that ISR/ATF4 activation disrupted HIV from latency. Of interest, when ISR/ATF4 signaling was prolonged, it also reduced HIV reservoir by depletion of replication-competent HIV. Importantly, such ISR/ATF4 signaling can be further enhanced when its negative regulatory feedback mechanism was additionally targeted. These observations indicate that the suppression of ISR signaling is associated with both latent HIV infection and the survival of HIV latently infected CD4⁺T cells.

Transient ISR activation temporarily pauses protein translation to correct misfolded or unfolded proteins or prevent pathogen infection, which is protective for the host cells for their survival.[14] When ISR is prolonged
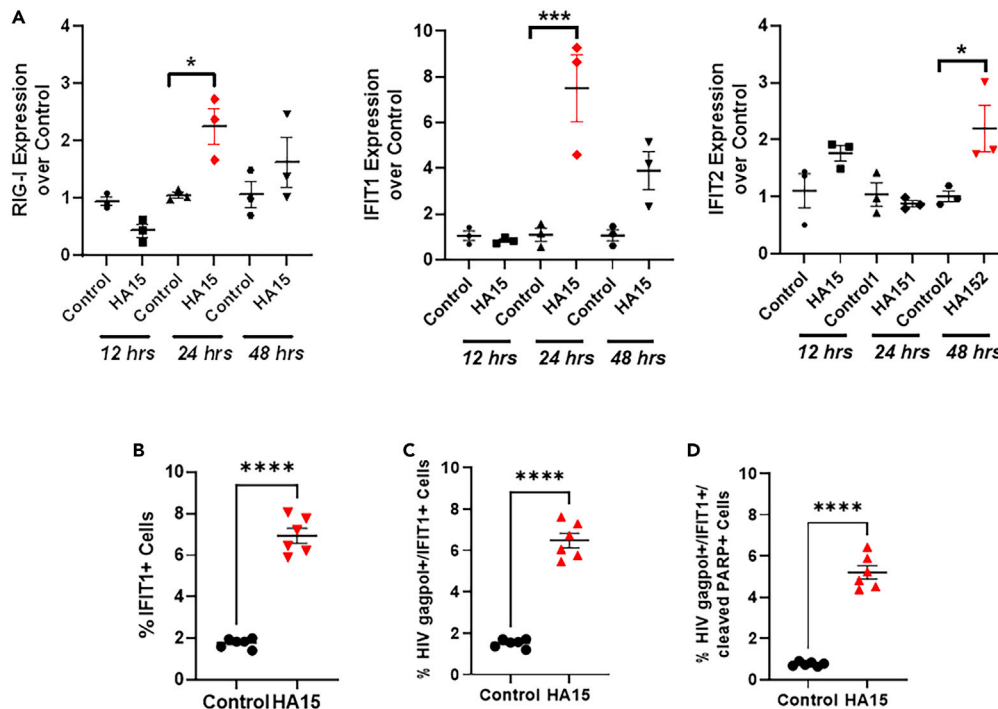
Figure 8. ISR/ATF4 activation by HA15 activates anti-viral IFIT1/cell death signaling in primary CD4⁺T cell model of latency

The primary CD4⁺T cell model of latency was treated with or without 20 µM HA15 for 48 h. Cells were collected 12 h, 1 day, and 2 days after the treatment. Total RNA was isolated, and RT-qPCR was performed to analyze the expression of IFN-I/IFIT signaling genes.

(A) *, $p<0.05$; ***, $p<0.001$; analyzed with One-way ANOVA(n = 3).

(B–D) Primary CD4⁺T cell model are treated with DMSO or HA15 (20 µM) for 4 days. Cells are collected and prepared for HIV RNA FISH-Flow to determine the percentage of IFIT1+ cells (B). The percentage of IFIT+/HIV RNA+ cells and cell death (% of cleaved PARP1+) was determined by HIV RNA FISH-Flow (C and D). *, $p<0.05$; **, $p<0.01$; ***, $p<0.001$; ****, $p<0.0001$; analyzed with two-tailed t-test (n = 3–6).

or sustained, or when homeostasis or protein mis-folding is too severe to be re-imbalanced, cells enter apoptosis to be purged by ATF4/CHOP death signaling. Following prolonged ISR/ATF4 activation, caspase 3 cleavage was only observed in the HIV latency model (HIV+ while quiescent) but not in HIV negative CD4⁺T cells. In the rCD4+ T cells isolated from ART-suppressed PLWH, ATF4 and CHOP were induced which was associated with the reduction of HIV DNA and RNA while the autophagy genes, such as ATG5 and ATG7, were not significantly impacted. This may be the reason why HIV+ cells were reduced upon ISR/ATF4 activation: Activation of ATF4/CHOP death signaling in HIV+ CD4⁺T cells without the enhancement of the survival autophagy pathway. Intriguingly, a unique ferroptosis cell death pathway was identified by scRNA-seq analyses after ISR/ATF4 activation. It warrants further investigation to define whether ferroptosis is involved in the survival of stable HIV reservoir (Figure S7C).

Our study discovered a new link of innate immune response to the depletion of HIV+ cells, downstream of ISR/ATF4 signaling activation. As a thiazolidinedione analog compound,[15,25] HA15 induced an anti-viral innate immune response in the primary CD4⁺T cell model of latency in which IFIT1 and IFIT2 were induced, which was opposite to what we observed in the Jurkat model of latency in which IFIT1 and IFIT2 were reduced and HIV transcription was induced after ISR/ATF4 signaling. It is well established that IFIT signaling activation impacts viral RNA instability, block viral RNA translation initiation and/or induces apoptosis.[14,26] This was supported by the signaling pathways uncovered by our scRNA-seq analyses, which may further strengthen the reduction of HIV reservoirs in the primary CD4⁺T cells (Figure S7C). Whether ISR/ATF4 signaling activation degrades HIV RNA transcripts and/or blocks HIV RNA translation to control HIV reservoir warrants further investigation. Regardless, these data indicate that latent HIV infection not only invades ISR/ATF4/HIV LTR signaling for its quiescence[11,13] but also dys-regulates its downstream ATF4/IFIT/cell death pathway for its survival.

Taken together, our study supports a proof-of-concept that the interplay of suppressed ISR/ATF4 activation with dampened cell death signaling is associated with the stable latent HIV reservoir of CD4+T cells. Conversely, enforced ISR activation not only induces HIV transcription from latency but also elicits apoptosis of HIV+ CD4+ cells, thereby depleting HIV reservoir for the remission of HIV.

Limitations of the study

In this report, we show that latent HIV infection dampens ISR/ATF4 signaling for its persistence in primary CD4+T cells. When ISR/ATF4 signaling is re-ignited, HIV latency is disrupted. If ISR/ATF4 signaling is prolonged, HIV+ CD4+T cells can be eradicated. This study expands our previous findings regarding the role of ISR/ATF4 in the seeding of stable viral reservoirs.[11,13] Our new findings here are clinically relevant as there is a possibility that ISR/ATF4 activation by HA15 may overcome the persistent HIV infection, offering an additional strategy to reactivate HIV and selectively kill latently HIV infected cells.

There are some limitations in this study, which warrant further investigation. First, although both ATF4/CHOP death pathway and IFIT1/cell death signaling are involved in the reduction of HIV+ immune cells, these two pathways may interplay. Activation of anti-viral IFIT signaling may also lead to degradation of viral RNA and stalled HIV RNA translation.[27] A mechanistic study is needed to understand IFIT signaling during HIV reservoir reduction. Second, although ISR/ATF4 activation reduces HIV reservoir in rCD4+ cells isolated from PLWH on ART, the sample size remains small. A follow-up study with a larger sample size is needed to further validate these findings. Also, it remains unclear whether the duration of 4-day treatment of HA15 is optimal to reduce HIV reservoirs among different latently infected CD4+T cells. Third, scRNA-seq analysis identifies a unique cell death pathway, ferroptosis,[24] upon ISR/ATF4 activation. Given that the transcripts of some essential anti-ferroptosis genes are enriched, it may prevent an optimal reduction of HIV+ cells. Study of this unique cell death pathway may discover a new tool to attack stable HIV reservoirs. Forth, it is of interest that anti-viral IFIT signaling may be intact in primary CD4+T cell model of latency but impaired in transformed cells of Jurkat latency model. If true, it indicates that anti-viral IFIT signaling may prevent an efficient latency reversal in immune cells. It is unknown whether this is relevant to the ineffective latency disruption in patient immune cells observed in almost all the studies using the current generations of latency reversal agents.[3,30] It may be useful to directly target IFIT signaling to maximize latency reversal. Lastly, it is not known whether ISR/ATF4 signaling is involved in persistence of non-T cell HIV reservoirs, such as brain myeloid cells, the putative reservoir cells in the CNS. Characterizing the role of ISR/ATF4 signaling in the reservoir of brain myeloid cells may lead to alternative tools to eradicate HIV from the CNS.

STAR★METHODS

Detailed methods are provided in the online version of this paper and include the following:

- KEY RESOURCES TABLE
- RESOURCE AVAILABILITY
  - Lead contact
  - Materials availability
  - Data and code availability
- EXPERIMENTAL MODEL AND SUBJECT DETAILS
  - Cell models
  - Primary CD4+T cell isolation and cell-associated HIV RNA or DNA measurements
- METHOD DETAILS
  - Viral outgrowth assay to measure replication competent HIV in the rCD4+ T cell isolation
  - Immunoblot analysis
  - HIV gene expression by real-time PCR analysis or flow cytometry
  - HIV gag-pol RNA FISH-Flow
  - Single cell RNA-seq
- QUANTIFICATION AND STATISTICAL ANALYSIS

SUPPLEMENTAL INFORMATION

Supplemental information can be found online at https://doi.org/10.1016/j.isci.2022.105743.

AUTHOR CONTRIBUTIONS

G.J. conceived the study. D.L., L.M.W., and Y.T. performed the latency reversal and reservoir reduction experiments in HIV latency models *in vitro and ex vivo*. G.R.T., B.A., K.S.J., and N.M.A. coordinated the patient blood samples and/or isolated the rCD4+ T cells. S.D. supported the initial study. J.M.S. and G.J. analyzed the scRNA-seq data. D.M.M. and Q.L. provided necessary scientific advice. D.L. and G.J. assembled the data and wrote the manuscript. All authors read and revised initial draft and approved the manuscript.

DECLARATION OF INTERESTS

The authors declare no conflict of interests.

REFERENCES

1. Pierson, T., McArthur, J., and Siliciano, R.F. (2000). Reservoirs for HIV-1: mechanisms for viral persistence in the presence of antiviral immune responses and antiretroviral therapy. Annu. Rev. Immunol. *18*, 665–708. https://doi.org/10.1146/annurev.immunol.18.1.665.

2. Margolis, D.M., Archin, N.M., Cohen, M.S., Eron, J.J., Ferrari, G., Garcia, J.V., Gay, C.L., Goonetilleke, N., Joseph, S.B., Swanstrom, R., et al. (2020). Curing HIV: seeking to target and clear persistent infection. Cell *181*, 189–206. https://doi.org/10.1016/j.cell.2020.03.005.

3. Rodari, A., Darcis, G., and Van Lint, C.M. (2021). The current status of latency reversing agents for HIV-1 remission. Annu. Rev. Virol. *8*, 491–514. https://doi.org/10.1146/annurev-virology-091919-103029.

4. Deeks, S.G., Archin, N., Cannon, P., Collins, S., Jones, R.B., de Jong, M.A.W.P., Lambotte, O., Lamplough, R., Ndung'u, T., Sugarman, J., et al. (2021). Research priorities for an HIV cure: international AIDS society global scientific strategy 2021. Nat. Med. *27*, 2085–2098. https://doi.org/10.1038/s41591-021-01590-5.

5. Wong, L.M., and Jiang, G. (2021). NF-kappaB sub-pathways and HIV cure: a revisit. EBioMedicine *63*, 103159. https://doi.org/10.1016/j.ebiom.2020.103159.

6. Elsheikh, M.M., Tang, Y., Li, D., and Jiang, G. (2019). Deep latency: a new insight into a functional HIV cure. EBioMedicine *45*, 624–629. https://doi.org/10.1016/j.ebiom.2019.06.020.

7. Mousseau, G., and Valente, S.T. (2016). Didehydro-Cortistatin A: a new player in HIV-therapy? Expert Rev. Anti Infect. Ther. *14*, 145–148. https://doi.org/10.1586/14787210.2016.1122525.

8. Nixon, C.C., Mavigner, M., Sampey, G.C., Brooks, A.D., Spagnuolo, R.A., Irlbeck, D.M., Mattingly, C., Ho, P.T., Schoof, N., Cammon, C.G., et al. (2020). Systemic HIV and SIV latency reversal via non-canonical NF-kappaB signalling in vivo. Nature *578*, 160–165. https://doi.org/10.1038/s41586-020-1951-3.

9. Pache, L., Dutra, M.S., Spivak, A.M., Marlett, J.M., Murry, J.P., Hwang, Y., Maestre, A.M., Manganaro, L., Vamos, M., Teriete, P., et al. (2015). BIRC2/cIAP1 is a negative regulator of HIV-1 transcription and can Be targeted by smac mimetics to promote reversal of viral latency. Cell Host Microbe *18*, 345–353. https://doi.org/10.1016/j.chom.2015.08.009.

10. Cosnefroy, O., Jaspart, A., Calmels, C., Parissi, V., Fleury, H., Ventura, M., Reigadas, S., and Andréola, M.L. (2013). Activation of GCN2 upon HIV-1 infection and inhibition of translation. Cell. Mol. Life Sci. *70*, 2411–2421. https://doi.org/10.1007/s00018-013-1272-x.

11. Jiang, G., Santos Rocha, C., Hirao, L.A., Mendes, E.A., Tang, Y., Thompson, G.R., 3rd, Wong, J.K., and Dandekar, S. (2017). HIV exploits antiviral host innate GCN2-ATF4 signaling for establishing viral replication early in infection. mBio *8*. 015188-16. https://doi.org/10.1128/mBio.01518-16.

12. Costa-Mattioli, M., and Walter, P. (2020). The integrated stress response: from mechanism to disease. Science *368*, eaat5314. https://doi.org/10.1126/science.aat5314.

13. Vallejo-Gracia, A., Chen, I.P., Perrone, R., Besnard, E., Boehm, D., Battivelli, E., Tezil, T., Krey, K., Raymond, K.A., Hull, P.A., et al. (2020). FOXO1 promotes HIV latency by suppressing ER stress in T cells. Nat. Microbiol. *5*, 1144–1157. https://doi.org/10.1038/s41564-020-0742-9.

14. Tian, X., Zhang, S., Zhou, L., Seyhan, A.A., Hernandez Borrero, L., Zhang, Y., and El-Deiry, W.S. (2021). Targeting the integrated stress response in cancer therapy. Front. Pharmacol. *12*, 747837. https://doi.org/10.3389/fphar.2021.747837.

15. Cerezo, M., Lehraiki, A., Millet, A., Rouaud, F., Plaisant, M., Jaune, E., Botton, T., Ronco, C., Abbe, P., Amdouni, H., et al. (2016). Compounds triggering ER stress exert anti-melanoma effects and overcome BRAF inhibitor resistance. Cancer Cell *29*, 805–819. https://doi.org/10.1016/j.ccell.2016.04.013.

16. Bradley, T., Ferrari, G., Haynes, B.F., Margolis, D.M., and Browne, E.P. (2018). Single-cell analysis of quiescent HIV infection reveals host transcriptional profiles that regulate proviral latency. Cell Rep. *25*, 107–117.e3. https://doi.org/10.1016/j.celrep.2018.09.020.

17. Li, D., Dewey, M.G., Wang, L., Falcinelli, S.D., Wong, L.M., Tang, Y., Browne, E.P., Chen, X., Archin, N.M., Margolis, D.M., and Jiang, G. (2022). Crotonylation sensitizes IAPi-induced disruption of latent HIV by enhancing p100 cleavage into p52. iScience *25*, 103649. https://doi.org/10.1016/j.isci.2021.103649.

18. Sahu, G.K., Lee, K., Ji, J., Braciale, V., Baron, S., and Cloyd, M.W. (2006). A novel in vitro system to generate and study latently HIV-infected long-lived normal CD4+ T-lymphocytes. Virology 355, 127–137. https://doi.org/10.1016/j.virol.2006.07.020.

19. De Gassart, A., Bujisic, B., Zaffalon, L., Decosterd, L.A., Di Micco, A., Frera, G., Tallant, R., and Martinon, F. (2016). An inhibitor of HIV-1 protease modulates constitutive eIF2alpha dephosphorylation to trigger a specific integrated stress response. Proc. Natl. Acad. Sci. USA 113, E117–E126. https://doi.org/10.1073/pnas.1514076113.

20. del Pino, J., Jiménez, J.L., Ventoso, I., Castelló, A., Muñoz-Fernández, M.Á., de Haro, C., and Berlanga, J.J. (2012). GCN2 has inhibitory effect on human immunodeficiency virus-1 protein synthesis and is cleaved upon viral infection. PLoS One 7, e47272. https://doi.org/10.1371/journal.pone.0047272.

21. Baxter, A.E., Niessl, J., Fromentin, R., Richard, J., Porichis, F., Massanella, M., Brassard, N., Alsahafi, N., Routy, J.P., Finzi, A., et al. (2017). Multiparametric characterization of rare HIV-infected cells using an RNA-flow FISH technique. Nat. Protoc. 12, 2029–2049. https://doi.org/10.1038/nprot.2017.079.

22. Tang, D., Chen, X., Kang, R., and Kroemer, G. (2021). Ferroptosis: molecular mechanisms and health implications. Cell Res. 31, 107–125. https://doi.org/10.1038/s41422-020-00441-1.

23. Cao, J.Y., and Dixon, S.J. (2016). Mechanisms of ferroptosis. Cell. Mol. Life Sci. 73, 2195–2209. https://doi.org/10.1007/s00018-016-2194-1.

24. Li, J., Cao, F., Yin, H.L., Huang, Z.J., Lin, Z.T., Mao, N., Sun, B., and Wang, G. (2020). Ferroptosis: past, present and future. Cell Death Dis. 11, 88. https://doi.org/10.1038/s41419-020-2298-2.

25. Trabattoni, D., Gnudi, F., Ibba, S.V., Saulle, I., Agostini, S., Masetti, M., Biasin, M., Rossignol, J.F., and Clerici, M. (2016). Thiazolides elicit anti-viral innate immunity and reduce HIV replication. Sci. Rep. 6, 27148. https://doi.org/10.1038/srep27148.

26. Diamond, M.S., and Farzan, M. (2013). The broad-spectrum antiviral functions of IFIT and IFITM proteins. Nat. Rev. Immunol. 13, 46–57. https://doi.org/10.1038/nri3344.

27. Pichlmair, A., Lassnig, C., Eberle, C.A., Górna, M.W., Baumann, C.L., Burkard, T.R., Bürckstümmer, T., Stefanovic, A., Krieger, S.,

Bennett, K.L., et al. (2011). IFIT1 is an antiviral protein that recognizes 5′-triphosphate RNA. Nat. Immunol. 12, 624–630. https://doi.org/10.1038/ni.2048.

28. Li, D., and Swaminathan, S. (2019). Human IFIT proteins inhibit lytic replication of KSHV: a new feed-forward loop in the innate immune system. PLoS Pathog. 15, e1007609. https://doi.org/10.1371/journal.ppat.1007609.

29. Fensterl, V., and Sen, G.C. (2015). Interferon-induced Ifit proteins: their role in viral pathogenesis. J. Virol. 89, 2462–2468. https://doi.org/10.1128/JVI.02744-14.

30. Grau-Expósito, J., Luque-Ballesteros, L., Navarro, J., Curran, A., Burgos, J., Ribera, E., Torrella, A., Planas, B., Badía, R., Martin-Castillo, M., et al. (2019). Latency reversal agents affect differently the latent reservoir present in distinct CD4+ T subpopulations. PLoS Pathog. 15, e1007991. https://doi.org/10.1371/journal.ppat.1007991.

31. Yukl, S.A., Kaiser, P., Kim, P., Telwatte, S., Joshi, S.K., Vu, M., et al. (2018). HIV latency in isolated patient CD4$^+$ T cells may be due to blocks in HIV transcriptional elongation, completion, and splicing. Sci. Transl. Med. 10, eaap9927. https://doi.org/10.1126/scitranslmed.aap9927.

32. Malnati, M.S., Scarlatti, G., Gatto, F., Salvatori, F., Cassina, G., Rutigliano, T., et al. (2008). A universal real-time PCR assay for the quantification of group-M HIV-1 proviral load. Nat. Protoc. 3, 1240–1248. https://doi.org/10.1038/nprot.2008.108.

33. Bruner, K.M., Wang, Z., Simonetti, F.R., et al. (2019). A quantitative approach for measuring the reservoir of latent HIV-1 proviruses. Nature 566, 120–125. https://doi.org/10.1038/s41586-019-0898-8.

34. Jordan, A., Bisgrove, D., and Verdin, E. (2003). HIV reproducibly establishes a latent infection after acute infection of T cells in vitro. EMBO J. 22, 1868–1877. https://doi.org/10.1093/emboj/cdg188.

35. Pearson, R., Kim, Y.K., Hokello, J., Lassen, K., Friedman, J., Tyagi, M., and Karn, J. (2008). Epigenetic silencing of human immunodeficiency virus (HIV) transcription by formation of restrictive chromatin structures at the viral long terminal repeat drives the progressive entry of HIV into latency. J. Virol. 82, 12291–12303. https://doi.org/10.1128/JVI.01383-08.

36. Jiang, G., Nguyen, D., Archin, N.M., Yukl, S.A., Méndez-Lagares, G., Tang, Y., Elsheikh, M.M., Thompson, G.R., 3rd, Hartigan-O'Connor, D.J., Margolis, D.M., et al. (2018). HIV latency is reversed by ACSS2-driven histone crotonylation. J. Clin. Invest. 128, 1190–1198. https://doi.org/10.1172/JCI98071.

37. Jiang, G., Maverakis, E., Cheng, M.Y., Elsheikh, M.M., Deleage, C., Méndez-Lagares, G., Shimoda, M., Yukl, S.A., Hartigan-O'Connor, D.J., Thompson, G.R., 3rd, et al. (2019). Disruption of latent HIV in vivo during the clearance of actinic keratosis by ingenol mebutate. JCI Insight 4, e126027. https://doi.org/10.1172/jci.insight.126027.

38. Jiang, G., Mendes, E.A., Kaiser, P., Wong, D.P., Tang, Y., Cai, I., Fenton, A., Melcher, G.P., Hildreth, J.E.K., Thompson, G.R., et al. (2015). Synergistic reactivation of latent HIV expression by ingenol-3-angelate, PEP005, targeted NF-kB signaling in combination with JQ1 induced p-TEFb activation. PLoS Pathog. 11, e1005066. https://doi.org/10.1371/journal.ppat.1005066.

39. He, D., Zakeri, M., Sarkar, H., Soneson, C., Srivastava, A., and Patro, R. (2022). Alevin-fry unlocks rapid, accurate and memory-frugal quantification of single-cell RNA-seq data. Nat. Methods 19, 316–322. https://doi.org/10.1038/s41592-022-01408-3.

40. Zhu, A., Srivastava, A., Ibrahim, J.G., Patro, R., and Love, M.I. (2019). Nonparametric expression analysis using inferential replicate counts. Nucleic Acids Res. 47, e105. https://doi.org/10.1093/nar/gkz622.

41. Hippen, A.A., Falco, M.M., Weber, L.M., Erkan, E.P., Zhang, K., Doherty, J.A., Vähärautio, A., Greene, C.S., and Hicks, S.C. (2021). miQC: an adaptive probabilistic framework for quality control of single-cell RNA-sequencing data. PLoS Comput. Biol. 17, e1009290. https://doi.org/10.1371/journal.pcbi.1009290.

42. Stuart, T., Butler, A., Hoffman, P., Hafemeister, C., Papalexi, E., Mauck, W.M., 3rd, Hao, Y., Stoeckius, M., Smibert, P., and Satija, R. (2019). Comprehensive integration of single-cell data. Cell 177, 1888–1902.e21. https://doi.org/10.1016/j.cell.2019.05.031.

43. Kolberg, L., Raudvere, U., Kuzmin, I., Vilo, J., and Peterson, H. (2020). gprofiler2 – an R package for gene list functional enrichment analysis and namespace conversion toolset g:Profiler. F1000Res. 9. ELIXIR-709. https://doi.org/10.12688/f1000research.24956.2.

STAR★METHODS

KEY RESOURCES TABLE

REAGENT or RESOURCE	SOURCE	IDENTIFIER
Antibodies		
anti-ATF4	Cell Signaling Technology	Cat#11815
anti-Caspase-3	Cell Signaling Technology	Cat#9662
anti-CHOP	Cell Signaling Technology	Cat#5554
anti-actin	Cell Signaling Technology	Cat#4970
anti-GAPDH	Cell Signaling Technology	Cat#2118
anti-LC3B	Invitrogen	Cat#L10382
IFIT1 (D2X9Z) Rabbit mAb (Pacific Blue™ Conjugate)	Cell Signaling Technology	Cat#96740
PE Mouse Anti-Cleaved PARP1 (Asp214)	BD Biosciences	Cat#552596
Biological samples		
Leukapheresis from HIV-infected individuals	University of North Carolina Hospital	N/A
Chemicals, peptides, and recombinant proteins		
HA15	Selleckchem	Cat#S8299
Sephin1	Cayman	Item#17757
Raltegravir	NIH AIDS Reagents Repository	N/A
Nevirapine	NIH AIDS Reagents Repository	N/A
Ritonavir	NIH AIDS Reagents Repository	N/A
Typan Blue stain 0.4%	Invitrogen	Cat#T10282
Recombinat Human IL-2	PEPROTECH	Cat#200-02
Critical commercial assays		
Protease/Phosphatase Inhibitor Cocktail (100X)	Cell signaling	Cat#5872
RNeasy mini kit	Qiagen	Cat#74106
DNase I	Invitrogen	Cat#18047019
SuperScript™ III Reverse Transcriptase	Invitrogen	Cat#18080093
TaqMan™ Universal PCR Master Mix	ABI	Cat# 4304437
EasySep™ Human CD4$^+$ T Cell Enrichment Kit	Stemcell Tech.	Cat#19052
EasySep™ Human Resting CD4$^+$ T Cell Isolation Kit	Stemcell Tech.	Cat#17962
LIVE/DEAD™ Fixable Far Red Dead Cell Stain Kit	Invitrogen	Cat#L34973
PrimeFlow™ RNA Assay Kit	Invitrogen	Cat#88-18005-210
eBioscience Annexin V Apoptosis Detection Kit eFluor 450	Invitrogen	Cat#88-8006
Experimental models: Cell lines		
Jurkat	ATCC	TIB-152
2D10	Jonathan Karn's lab	N/A
J-Lat A1	NIH AIDS Reagents Repository	N/A
Primary CD4$^+$ T cell model of latency	Ed Browne lab	E47
Oligonucleotides		
HIV LTR probe: 6FAMCCA GAG TCA CAC AAC AGA CGG GCA CAT AMRA	Invitrogen	Steven A. Yukl, et al. 2018.[31]
HIV LTR sense: GCC TCA ATA AAG CTT GCC TTG A	Invitrogen	Steven A. Yukl, et al. 2018.[31]
HIV LTR antisense: GGG CGC CAC TGC TAG AGA	Invitrogen	Steven A. Yukl, et al. 2018.[31]
HIV gag FWD: TACTGACGCTCTCGCACC	Invitrogen	Malnati et al., 2008[32]

Continued

REAGENT or RESOURCE	SOURCE	IDENTIFIER
HIV gag REV: TCTCGACGCAGGACTCG	Invitrogen	Malnati et al., 2008[32]
HIV gag probe: FAM-CTCTCTCCTTCTAGCCTC	Invitrogen	Malnati et al., 2008[32]
HIV poly A FWD: gccctcagatgctrcatataa	Thermo Scientific	Steven A. Yukl et al., 2018[31]
HIV poly A REV: tttttttttttttttttttttttttttgaag	Thermo Scientific	Steven A. Yukl et al., 2018[31]
HIV poly A probe: tgcctgtactgggtctctctggttag	Thermo Scientific	Steven A. Yukl et al., 2018[31]
HIV ENV FWD: AGTGGTGCAGAGAGAAAAAAGAGC	Invitrogen	Bruner et al., 2019[33]
HIV ENV REV: GTCTGGCCTGTACCGTCAGC	Invitrogen	Bruner et al., 2019[33]
HIV ENV intact probe: CCTTGGGTTCTTGGGA	Invitrogen	Bruner et al., 2019[33]
HIV ENV hypermut probe: CCTTAGGTTCTTAGGAG	Invitrogen	Bruner et al., 2019[33]
GAPDH (Hs99999905_m1)	Thermo Scientific	Cat#4331182
ATF4 (Hs00909569_g1)	Thermo Scientific	Cat#4331182
CHOP (Hs00358796_g1 DDIT3)	Thermo Scientific	Cat#4331182
IFIT1 (Hs03027069_s1)	Thermo Scientific	Cat#4331182
IFIT2 (Hs00533665_m1)	Thermo Scientific	Cat#4331182
RIG-I (Hs01061444_m1 DDX58)	Thermo Scientific	Cat#4331182
STAT1 (Hs01013996_m1)	Thermo Scientific	Cat#4331182
STAT2 (Hs01013115_g1)	Thermo Scientific	Cat#4331182
STAT3 (Hs00374280_m1)	Thermo Scientific	Cat#4331182
ATG5 (Hs00355494_m1)	Thermo Scientific	Cat#4331182
ATG7 (Hs00893766_m1)	Thermo Scientific	Cat#4331182
MyD88 (Hs00182082_m1)	Thermo Scientific	Cat#4331182
MDA5 (Hs01070332_m1)	Thermo Scientific	Cat#4331182
IRF3 (Hs01547283_m1)	Thermo Scientific	Cat#4331182
IRF7 (Hs01014809_g1)	Thermo Scientific	Cat#4331182
SAMHD1 (Hs00210019_m1)	Thermo Scientific	Cat#4331182
Monkey eIF2a (Rh01045428_m1)	Applied Biosystems	Cat#4351372
Monkey GCN2 (Rh01010957_m1 EIF2AK4))	Applied Biosystems	Cat#4351372
Monkey ATF4 (Rh029266992_m1)	Applied Biosystems	Cat#4351372
Human TBP (Hs99999910_m1)	Applied Biosystems	Cat#4333769F
SDHA (Hs00188166_m1)	Thermo Scientific	Cat#4331182
PrimeFlow Type 6 probe set: HIV gag-pol	Thermo Scientific	Cat#VF6-11403
PrimeFlow Type 6 probe set: Human RPL 13A	Thermo Scientific	Cat#VF6-13186
PrimeFlow Type 6 probe set: Bacillus S dapb	Thermo Scientific	Cat#VF6-10407
Software and algorithms		
GraphPad Prism 8	GraphPad Software Inc.	https://www.graphpad.com/
FlowJo v9	BD	https://www.flowjo.com/

RESOURCE AVAILABILITY

Lead contact

Further information or requests for resources should be directed to the lead contact, Dr. Guochun Jiang at guochun_jiang@med.unc.edu. No new unique reagents were generated in this study.

Materials availability

The transfer of biological research materials are available under the Uniform Biological Material Transfer Agreement in NIH.

Data and code availability

Single-cell RNA-seq data were deposited to the Gene Expression Omnibus and raw and processed data are available under accession GSE: GSE210824. Code used to analyze single-cell data are available at https://github.com/jeremymsimon/Li_HIV_HA15.

EXPERIMENTAL MODEL AND SUBJECT DETAILS

Cell models

Jurkat cell model of HIV latency and derivatives, 2D10 and J-Lat A1 cells, were cultured in RPMI 1640 medium with 10% fetal bovine serum (FBS) and 1% penicillin streptomycin (Pen-Strep) in 37°C incubator containing 5% CO_2. Jurkat and J-Lat A1 cells were from NIH AIDS Reagents Repository while 2D10 cell model of latency was a gift from Jonathan Karn's lab. The J-Lat A1 model of HIV latency contains one copy of a construct containing HIV-LTR-driven Tat and green fluorescent protein (GFP) gene in Jurkat T cells.[34] The 2D10 model of HIV latency carries a lentiviral vector that expresses Tat with H13L mutation and Rev in cis and a destabilized green fluorescent protein (d2EGFP) in place of Nef.[35] HIV negative primary CD4+T cells (from UCLA CFAR) and primary CD4+T cell model of latency was also used.[16,17] Briefly, primary CD4+T cells were infected with pNL4.3Δ6-GFP. Then, GFP positive cells were sorted and then co-cultured with H80 feeder cells to allow the establishment of HIV latency. Later on, latently infected GFP- CD4+T cells were sorted and cultured as the primary CD4+T cell model of HIV latency.[16,17]

Primary CD4+T cell isolation and cell-associated HIV RNA or DNA measurements

Peripheral blood or leukapheresis samples were collected from HIV-positive individuals receiving suppressive ART for at least 3 years with undetectable viral loads. CD4+T cells were isolated using the EasySep CD4+T cells Enrichment Kit or a custom rCD4+ T cells isolation kit (StemCell Technologies).[11,36,37] The purified CD4+T cells were plated at a density of 1×10^6 cells with or without HA15 treatment. For the HIV DNA measurements in rCD4+ T cells from ART-suppressed individuals, 3–4 replicates of 2–5 million rCD4+ T cells per replicate were treated with compounds. Total DNA was isolated from harvested cells. Then, gag HIV env DNA was measured.[17] All the participants were provided informed consent, and the study was approved by the UC-Davis and UNC-Chapel Hill Institutional Review Boards.

METHOD DETAILS

Viral outgrowth assay to measure replication competent HIV in the rCD4+ T cell isolation

Resting CD4+T cells were purified as indicated above. The cells were treated with or without 20 μM HA15 for 4 days in the presence of ART+20 U/mL IL-2. Treatment and ART were washed out and the cells were treated with 2 μg/mL PHA for 24 hours in the presence of 20 U/mL IL-2. After removing PHA, the cells were co-culture with CD8-depleted PBMCs with 20 U/mL IL-2. The medium was changed every three days. Twenty one days post co-culture, the cells and supernatants were collected and cellfree HIV gag RNA, cell-associated HIV gag RNA and cell-associated HIV DNA were measured by droplet digital PCR (ddPCR)/RT-PCR with 3–4 replicates in each sample.

Immunoblot analysis

Whole cell protein extract or nuclear protein was prepared with RIPA lysis buffer (Sigma) containing 1x proteinase inhibitors and phosphatase inhibitors (Cell Signaling). Protein expression was evaluated using the following antibodies: anti-ATF4 (Cell Signaling), anti-β-actin (Cell Signaling), anti-GAPDH (Cell Signaling), anti-CHOP (Cell Signaling), anti-LC3B (Cell Signaling), and anti-caspase3 (Cell Signaling).

HIV gene expression by real-time PCR analysis or flow cytometry

Total RNA was isolated using the RNeasy kit (Qiagen) followed by digestion with DNase I (Invitrogen). First-strand cDNA was synthesized using Superscript III (Invitrogen) with random primers (Invitrogen). Real-time PCR (TaqMan) was performed on an ABI QuantStudio 5 system using primers/probe sets,[11,38] where HIV was amplified with the early gag/long LTR region of HIV. The glyceraldehyde-3-phosphate dehydrogenase (GAPDH) and SDHA primers/probe sets were used for control PCR (Applied Biosystems Inc.) or HIV (GFP) was quantified by GFP expression using flow cytometry and the data were analyzed using FlowJo Software. Cell viability was evaluated using trypan blue and Live/Dead dye (Life Technologies) during flow cytometry.

HIV gag-pol RNA FISH-Flow

This was followed by the manual of PrimeFlow™ RNA Assay Kit (Invitrogen) and has been published,[21] which described as below.

Cell collection, preparation and fixation I

After treatment, the cells were collected and washed with 1x PBS at 4 °C and fixed in Fixation Buffer I. Then, cells were washed twice with the Permeabilization Buffer.

Intracellular antibody stain and fixation II

Anti-cleaved PARP1 (PE-conjugated, BD) antibody, anti-IFIT1 antibody (Pacific blue-conjugated, Cell signaling), or both of anti-cleaved PARP1 plus anti-IFIT1 was added directly to the residual 100 μL sample in each tube. Mix by pipetting gently, incubate at 4°C for 1.5 hr in the dark. One milliliter of Permeabilization Buffer were added to the residual volume, and cells were collected at 800 xg for 5 min at 4 °C for washing. Then, add 1 mL of Fixation Buffer II (Room temperature, RT) to the 100 μL: residual volume and incubate for 1 hr at RT in the dark.

Labelling mRNA

During Fixation II, mRNA target probes were thawed at room temperature for the preparation of mRNA Target Probe Mixes in Target Diluent. The cells in Fixation Buffer 2 were centrifuged at 800 xg for 5 min at room temperature and washed twice in Wash Buffer at room temperature.100 μL of the warm Target Probe Mix were added into the 100 μL residual volume. Then, the samples were placed into a metal heat block within an oven pre-heated to 40 °C. Samples were incubated for 2 hr at 40 °C where halfway through incubation, samples were inverted once to mix gently. Then, the cells were washed with Wash Buffer for 3 times at room temperature.

Amplification

100 μL of the warm Pre-Amplification Mix were added into the 100 μL residual volume. Mix gently by pipetting until the two liquids no longer appear separate and incubate the samples for 1.5 hours at 40 °C. Cells were washed in Wash Buffer for 3 times at room temperature where 100 μL of the warm Amplification Mix were added into the 100 μL residual volume. Mix gently until the two liquids no longer appear separate and then incubate for 1.5 hr at 40 °C. Wash cells with Wash Buffer for 3 times at room temperature.

Labelling amplified signal

Prepare the Label Probe Mix where ensure the Label Probe diluent was at 40 °C before use. Add 100 μL of the warm Label Probe Mix into the 100 μL residual volume. Mix gently by pipetting. Incubate for 1 hour at 40 °C. Then, Wash cells with Wash Buffer for 3 times at room temperature.

Acquisition and sample compensation

Complete a final wash with either Storage Buffer or 2% FBS/PBS for acquisition on a flow cytometer. Sample compensation was prepared on day 1 of the assay with the kit Stain UltraComp eBeads™ microspheres (ThermoFisher Inc). Mix UltraComp eBeads™ microspheres by vigorously inverting at least 10 times or pulse-vortex. Add 1 drop of UltraComp eBeads™ microspheres to each compensation tube. For each RNA detection channel used, add 5 μL of the appropriate Compensation Control to the appropriate tube. For each experimental antibody used, add 1 test or less of conjugated antibody to the appropriate tube. Mix briefly by flicking or pulse-vortex. Incubate for 15–30 minutes at 2–8°C. Add 2 mL of Flow Cytometry Staining Buffer to each tube and spin down at 400–600 × g for 3–5 minutes at RT. Decant the supernatant and resuspend beads in the 100 μL residual volume by vortex gently. Add 100 μL of IC Fixation Buffer to each tube and briefly vortex to mix. Before acquiring on a cytometer, wash with 2 mL of Flow Cytometry Staining Buffer and re-suspend beads in the 0.2–0.4 mL of Flow Cytometry Staining Buffer to each tube.

Single cell RNA-seq

Single cell RNA-seq was performed by the Advanced Analytics core at UNC-Chapel Hill. Briefly, the primary CD4^{+}T cells of HIV latency were treated with or without 20 μM HA15 for 2 days. The single cell suspensions were prepared and loaded on a GemCode Single-Cell instrument (10X Genomics, Pleasanton, CA) to generate single-cell beads in emulsion. All 3 replicates of each condition were multiplexed using hashtag

oligos (Biolegend). Then, scRNA-seq libraries were prepared using GemCode Single Cell 3′ Gel bead and library kit (10X Genomics) and quantified by quantitative PCR (Kappa Biosystems, Wilmington, MA) and sequenced on an Illumina NovaSeq 6000-SP (San Diego CA). Read lengths were 28 bp for read 1, 10 bp i7 index, 10 bp for i5 index and 90 bp read 2. The flowcell was run in XP mode over both lanes. Hashtag oligo and gene expression was computed and cells were deconvoluted using alevin-fry[39] using a 'splici' reference genome constructed using the concatenated hg38 and HIV genomes and GENCODE v36 transcriptomes. Hashtag oligo and gene expression data were then imported into R v4.1 using fishpond,[40] and hashtag oligos were demultiplexed using Seurat HTODemux. Cells were filtered if they contained a significant contribution of mitochondrial transcript signal using miQC,[41] and subsequently filtered to contain at least 2,000 UMIs and at least 1,000 detected genes per cell. Gene expression data were then normalized using scTransform v2 and samples were integrated together to identify one joint collection of cell clusters using Seurat[42] with Louvain-Jaccard clustering with multilevel refinement (resolution = 0.25). Differential expression between HA15 and control-treated cells was performed using Distinct using log2 CPM (p_adj.glb <0.05),[43] and significant pathway enrichment was identified using g:Profiler focusing on KEGG and REACTOME pathways (FDR <0.05).[43]

QUANTIFICATION AND STATISTICAL ANALYSIS

Data were presented as mean $\pm$ SEM which were collected from at least three independent experiments. Statistical analysis was performed using Prism GraphPad 9.1. Significance was determined by One-way ANOVA for multiple comparisons or by student t-test for two groups where $p < 0.05$ considered significance.